Biochimica et Biophysica Acta 1817 (2012) 66–75

Contents lists available at SciVerse ScienceDirect

Biochimica et Biophysica Acta

journal homepage: www.elsevier.com/locate/bbabio

Review

Cytochrome b_{559} and cyclic electron transfer within photosystem II ☆

Katherine E. Shinopoulos, Gary W. Brudvig *

Department of Chemistry, Yale University, New Haven, CT 06520-8107, USA

ARTICLE INFO

Article history:
Received 25 May 2011
Received in revised form 6 August 2011
Accepted 8 August 2011
Available online 16 August 2011

Keywords:
β-Carotene
Chlorophyll
Cytochrome b_{559}
Electron transfer pathway
Photosystem II

ABSTRACT

Cytochrome b_{559} (Cyt b_{559}), β-carotene (Car), and chlorophyll (Chl) cofactors participate in the secondary electron-transfer pathways in photosystem II (PSII), which are believed to protect PSII from photodamage under conditions in which the primary electron-donation pathway leading to water oxidation is inhibited. Among these cofactors, Cyt b_{559} is preferentially photooxidized under conditions in which the primary electron-donation pathway is blocked. When Cyt b_{559} is preoxidized, the photooxidation of several of the 11 Car and 35 Chl molecules present per PSII is observed. In this review, the discovery of the secondary electron donors, their structures and electron-transfer properties, and progress in the characterization of the secondary electron-transfer pathways are discussed. This article is part of a Special Issue entitled: Photosystem II.

1. Introduction

Photosystem II (PSII) catalyzes the first step of oxygenic photosynthesis in which electrons are extracted from water, ultimately resulting in conversion of energy from the sun into chemical energy. Each time the energy from a photon of light reaches the reaction center of PSII, a charge separation occurs from a group of four chlorophylls denoted as P_A, P_B, B_A and B_B (Fig. 1); the primary electron donor is called P_{680}. The electron is transferred to a membrane-bound quinone, Q_A, via a pheophytin ($Pheo_A$) cofactor. The charge separation between P_{680} and Q_A, 26 Å apart, is long-lived with a time constant for recombination of at least 0.1 ms in higher plants [1–4] and 1 ms in cyanobacteria [2,5–9]. During electron transfer that results in water-oxidation catalysis, the hole remaining on P_{680} is transferred to the catalytic tetra-manganese cluster known as the oxygen-evolving complex (OEC) via a redox-active tyrosine, Y_Z, and the electron on Q_A is transferred to the terminal electron acceptor in PSII, Q_B (reviewed in [10]). The OEC stores the oxidizing potential, cycling in single electron-transfer steps from S_0 (the least oxidized state) to S_4 (the most oxidized state), when it is capable of splitting water into O_2, electrons, and protons. However, when $P_{680}^{\bullet+}$, with a reduction potential of about 1.25 V [11,12], cannot oxidize the primary electron donors of PSII, which include Y_Z and the OEC, photoinhibition resulting in loss of activity can occur (reviewed in [13]). Potential sources of photoinhibition include oxidative damage to proteins and cofactors, or recombination of the $P_{680}^{\bullet+}Q_A^{\bullet-}$ radical pair, forming $^3P_{680}$ that can sensitize the formation of singlet oxygen and other reactive oxygen species [14–18].

Under conditions in which electron transfer from the OEC is impaired, photooxidation of the redox-active tyrosine in the D2 subunit (Y_D), β-carotene (Car), chlorophyll (Chl), and cytochrome (Cyt) b_{559} has been observed (Fig. 1). These secondary pathways of electron transfer have been proposed to protect PSII from oxidative photodamage under high light conditions or while the OEC is undergoing assembly [19]. An oxidizing equivalent on Y_D does not equilibrate among the other secondary electron donors and, as such, Y_D serves as a singular secondary electron donor and typically remains oxidized under steady-state illumination of PSII. On the other hand, an oxidizing equivalent rapidly equilibrates among Cyt b_{559}, Car, and Chl [20]. As the lowest potential donor, Cyt b_{559} is preferentially oxidized when an oxidizing equivalent from $P_{680}^{\bullet+}$ equilibrates among these secondary electron donors. Oxidized Cyt b_{559} is then capable of accepting an electron from a reduced plastoquinone (PQ) on the electron acceptor side of PSII, thus forming a cyclic pathway of electron transfer that connects the donor and acceptor sides of PSII to remove excess oxidizing equivalents (see Section 2).

The one copy of Cyt b_{559} per PSII is located near the D2 subunit (Fig. 1A), slightly separated from the primary electron-transfer

Abbreviations: ADRY, acceleration of the deactivation reactions of the water-splitting system Y; Car, β-carotene; $Car^{\bullet+}$, oxidized Car; CD, circular dichroism; Chl, chlorophyll; $Chl^{\bullet+}$, oxidized Chl; Chl_{ZD1}/Chl_{ZD2}, redox-active Chl in the D1/D2 polypeptides; CP43/CP47, 43/47 kDa chlorophyll binding proteins in PSII; Cyt, cytochrome; D1/D2, homologous PSII reaction center core proteins; ENDOR, electron nuclear double resonance; EPR, electron paramagnetic resonance; ESEEM, electron spin echo envelope modulation; FTIR, Fourier transform infrared; HP, high potential; HPLC, high performance liquid chromatography; HYSCORE, hyperfine sub-level correlation; IP, intermediate potential; LD, linear dichroism; LP, low potential; Near-IR, near-infrared; OEC, oxygen-evolving complex; P_{680}, primary Chl electron donor in PSII; Pheo, pheophytin; PQ, plastoquinone; PSII, photosystem II; Q_A/Q_B, redox-active quinones bound to PSII; $S_0/S_1/S_2/S_3/S_4$, the redox states of the OEC; WT, wild type; Y_Z/Y_D, redox active tyrosines in the D1/D2 polypeptides

☆ This article is part of a Special Issue entitled: Photosystem II.

* Corresponding author. Tel.: +1 203 432 5202; fax: +1 203 432 6144.
E-mail address: gary.brudvig@yale.edu (G.W. Brudvig).

0005-2728/$ – see front matter © 2011 Elsevier B.V. All rights reserved.
doi:10.1016/j.bbabio.2011.08.002

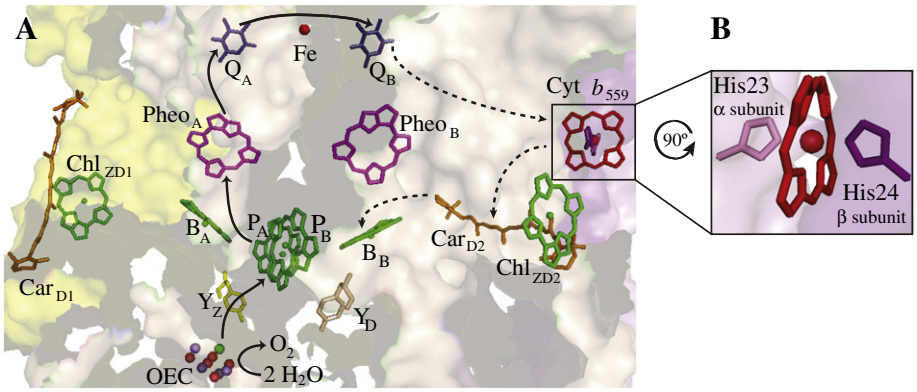

Fig. 1. A. Electron-transfer cofactors in photosystem II, viewed from along the membrane plane (PDB ID: 3ARC), with solid arrows showing the primary electron-transfer steps and dashed arrows showing secondary electron-transfer pathways. The oxygen-evolving complex (OEC) is shown with manganese atoms in purple, oxygen in red, and calcium in green; tyrosine Z (Y_Z) is shown in yellow and tyrosine D (Y_D) is shown in tan; chlorophylls (Chl) are shown in green; β-carotene (Car) is shown in orange; pheophytins ($Pheo_A$ and $Pheo_B$) are shown in magenta; and quinones (Q_A and Q_B) are shown in blue. The surfaces of the D1, D2, α- and β-Cyt b_{559} subunits are colored yellow, tan, pink and purple, respectively. B. An enlarged view of Cyt b_{559}.

cofactors. The heme is ligated via two His residues, one each from the α and β Cyt b_{559} subunits, thereby forming a cross-linked structure (Fig. 1B). Cyt b_{559} displays a range of midpoint potentials depending on the type of PSII preparation and treatment: −150–0 mV (low potential or LP), +230 mV (intermediate potential or IP), and +390 mV (high potential or HP) (see Section 3). The structural differences among the different forms of Cyt b_{559} are unknown, and while many treatments have been observed to shift Cyt b_{559} from the HP to LP form *in vitro*, the restoration of the HP form is more difficult to achieve experimentally. However, it has been hypothesized that the interconversion may play a physiological role in mediating the operational type of photoprotection (see Section 2.1).

The connectivity and sequence of electron-transfer events among Cyt b_{559} and the multiple redox-active Car and Chl are of interest in understanding the characteristics of secondary electron transfer and its physiological relevance. Crystallographic studies have yielded detailed information on the structure of PSII and the locations of the cofactors (see Section 4); however, the redox-active cofactors must be identified by other spectroscopic methods (see Section 2). Recent studies have characterized secondary electron transfer under a variety of conditions, including in systems containing different redox forms of Cyt b_{559} and in both catalytically active (O_2 evolving) and inactive PSII samples (see Section 5). Other reviews provide additional information on the secondary donors [21–24] and Cyt b_{559} [19,25–27].

2. Spectroscopy identifying the cofactors involved in secondary electron transfer

2.1. The discovery of the redox activity of Cyt b_{559}

Although photosynthesis has been studied for more than a century, the redox-activity of the secondary cofactors, Car, Chl, and Cyt b_{559}, was discovered more recently. Photooxidation of the preferred electron donor in the secondary electron-transfer pathway, Cyt b_{559}, was observed by absorption spectroscopy at cryogenic temperatures [28,29]. An inverse relationship between Cyt b_{559} oxidation and S_2 state formation was observed by EPR spectroscopy, indicating that the two species are competing electron donors to $P_{680}^{\bullet+}$ [30]. Photooxidized Cyt b_{559} was also found to be photoreduced [31], and it was hypothesized that PQ was the source of electrons [26], creating a cyclic pathway around PSII hypothesized to decrease damage due to high light [32,33]. The presence of a cyclic pathway was confirmed at saturating light intensities by the greater yield of variable fluorescence, indicative of charge separation, than the yield of O_2 [34]. It was observed that the magnitude of photooxidation and photoreduction of Cyt b_{559} increased under stress conditions, such as high temperature, implying a biological role for the cyclic pathway in photoprotection [35].

At room temperature, the rate of photooxidation of Cyt b_{559} in O_2-evolving PSII samples ($t_{1/2} = 760 \pm 260$ ms at pH 6.0) is on the same order of magnitude as the rate of $S_2\ Q_A^{\bullet-}$ charge recombination [36], and the rate of Cyt b_{559} photooxidation in PSII samples inactive for O_2-evolution ($t_{1/2} = 13$ ms at pH 6.0) is similar to the rate of $Y_Z^{\bullet+}\ Q_A^{\bullet-}$ charge recombination [7]. However, a higher yield of oxidized Cyt b_{559} was detected in non-O_2-evolving PSII samples [7,35,36]. These observations were explained by a model where Cyt b_{559} is photooxidized via electron transfer from the reduced heme to $P_{680}^{\bullet+}$, which is present in equilibrium with either the S_2 state or $Y_Z^{\bullet+}$ [7,36].

Following its photooxidation, Cyt b_{559} photoreduction has also been observed at pH ≥ 6. In a sample of PSII-enriched membranes (BBY-type preparation), the $t_{1/2}$ is about 50 s [36], while in chloroplasts the $t_{1/2} = 100$ ms [26]. There have been several hypotheses regarding the source of the electrons, including the PQ pool [26], Q_B^- [36], or $Pheo^-$ [37–39]. Based on the 1.9 Å resolution crystal structure [40], electron transfer to Cyt b_{559} from the Q_B site, 25 Å away, may not be possible with a $t_{1/2}$ of 100 ms [21], although it would be possible with a $t_{1/2}$ of 50 s. Electron transfer from $Pheo^-$ to Cyt b_{559}, at a distance of 38 Å, would not be possible with either $t_{1/2}$. There are significant differences between samples composed of chloroplasts and of PSII-enriched membranes, including the size of the PQ pool, the condition of the Q_B site, and the presence or absence of gradients across the chloroplast membrane; also, the source of electrons may be different in the two samples.

Under some conditions, photoinhibition is decreased when LP Cyt b_{559} is preoxidized and available for reduction by the acceptor side of PSII [37–39,41]. However, increasing the amount of LP Cyt b_{559} has not yielded an appreciable decrease in photoinhibition at high light intensities [42]. Still, it has been hypothesized that HP and LP Cyt b_{559} may interconvert reversibly [41], with HP Cyt b_{559}, which is reduced under ambient conditions, poised to donate an electron to $P_{680}^{\bullet+}$ under donor-side stress, and LP Cyt b_{559}, which is predominantly oxidized under ambient conditions, poised to accept an electron under acceptor-side stress in which excess electrons accumulate on Q_A and Pheo [37–39,41,43].

2.2. Observations of $Chl^{\bullet+}$ and $Car^{\bullet+}$ before 2000

The photobleaching of neutral Car [44] and Chl [45] was first observed in chloroplasts with illumination under oxidizing conditions. Later, flash-induced absorbance changes showed Car bleaching concomitant with Cyt b_{559} reduction at room temperature in the presence of an ADRY reagent, which disrupts normal electron transfer [46]. $Car^{\bullet+}$ was also observed by flash absorption spectroscopy at room

temperature in the presence of phenolic herbicides with a $t_{1/2} = 10$–35 μs [47]. At cryogenic temperature, it was shown that Car bleaching occurred without ADRY reagents or herbicides, and was due to $Car^{\bullet+}$ formation, marked by an absorbance peak at 990 nm (see Fig. 3) in conjunction with bleaching at 480 nm [48]. Samples with preoxidized Cyt b_{559} yielded a greater absorbance at 990 nm, providing a clue that Car and Cyt b_{559} are members of the same electron-transfer pathway [48]. This was reinforced by the detection of an EPR signal attributed to $Chl^{\bullet+}$ or $Car^{\bullet+}$ present only in samples with Cyt b_{559} preoxidized [30,49]. Additionally, Chl (or Car) and Cyt b_{559} demonstrated the same rate of electron transfer to $P_{680}^{\bullet+}$, shown by similar relative yields of their EPR spectra compared to the S_2 state spectrum at cryogenic temperature, indicating that Cyt b_{559} donates an electron to $P_{680}^{\bullet+}$ through an intermediate, redox-active Chl or Car, and that the slower step is donation to $P_{680}^{\bullet+}$ [33].

However, it has been suggested [21] that the increasing oxidation of the secondary donors compared to S_2 state formation as the temperature is decreased is not a result of competing rates, but instead a result of freezing PSII in conformations in which Y_Z cannot be oxidized and thus the S_2 state cannot be formed. In this population of centers, the oxidation of secondary donors competes with the slower rate of $P_{680}^{\bullet+}Q_A^{\bullet-}$ charge recombination ($t_{1/2}$ ~ 1–5 ms at cryogenic temperature), and not Y_Z donation ($t_{1/2} = 4.2$ μs) [8,21].

Further characterization of $Car^{\bullet+}$ and $Chl^{\bullet+}$ was subsequently obtained from spectroscopy on a variety of sample types. PSII-enriched membranes from higher plants contain all of the subunits of PSII, as well as peripheral LHC-II light harvesting complexes. PSII isolated from *Synechocystis* contains all of the PSII subunits present in that species, without any peripheral light harvesting complexes. Samples of PSII reaction centers contain only the D1/D2/Cyt b_{559} subunits and a limited number of pigments. PSII reaction center preparations can carry out the primary charge separation between P_{680} and Pheo; however, these preparations are unable to photooxidize Y_Z or Y_D, do not contain Q_A or Q_B, and have different portions of the protein exposed to solvent, potentially perturbing the redox potentials of the cofactors.

In PSII reaction centers, absorption spectroscopy showed the oxidation of Car [50], in addition to Chl [51], with bleaching of Car occurring more rapidly, and modification of neutral pigments was shown by HPLC [50]. The Car bleaching was also biphasic, implying that two Car were oxidized, one more rapidly than the other [50]. $Chl^{\bullet+}$ and $Car^{\bullet+}$ were also detected by FTIR spectroscopy on PSII-enriched membranes [52], and by ENDOR spectroscopy on both PSII-enriched membranes and PSII reaction centers [53]. Fluorescence spectroscopy on PSII-enriched membranes indicated that $Chl^{\bullet+}$ is a strong quencher of fluorescence with implications for photoprotection under high light [54]. Resonance Raman spectroscopy was performed on PSII reaction centers [55] and on PSII isolated from *Synechocystis* [56,57], where the observation that Cyt b_{559} must be pre-oxidized to observe $Chl^{\bullet+}$ and $Car^{\bullet+}$ indicated that these cofactors are members of the same electron-transfer pathway [57]. Electron transfer along this pathway was observed experimentally in PSII-enriched membranes solubilized with 0.5% β-DM, where $Car^{\bullet+}$ formed by illumination at liquid helium temperatures was converted into $Chl^{\bullet+}$ upon warming [58], although the electron transfer may have been modified by the presence of detergent [20,59].

Unfortunately, $Chl^{\bullet+}$ and $Car^{\bullet+}$ sometimes have similar spectral signatures, including their 9 GHz (X-band) EPR spectra [57,60,61], and there has historically been some confusion regarding the conditions that result in the formation of $Chl^{\bullet+}$, $Car^{\bullet+}$, or both (see introduction in ref. [58]). Generally, it is true that illumination at low temperatures with preoxidized Cyt b_{559} generates both the $Car^{\bullet+}$ $Q_A^{\bullet-}$ and $Chl^{\bullet+}$ $Q_A^{\bullet-}$ charge separations from at least 6 to 190 K [20,60], and that $Chl^{\bullet+}$ $Q_A^{\bullet-}$ is more stable than $Car^{\bullet+}$ $Q_A^{\bullet-}$ as the temperature increases. Currently, $Chl^{\bullet+}$ and $Car^{\bullet+}$ can be distinguished by several forms of spectroscopy, including high-field EPR [60,61] and near-IR absorption (see Section 5), among others.

3. Properties of Cyt b_{559}

Cyt b_{559} is composed of one α- and one β-subunit, each providing one His ligand to the heme (shown in Fig. 1B), and is an integral part of PSII adjacent to the D2 subunit [62]. Interestingly, Cyt b_{559} displays a range of redox potentials in PSII, from −150 to +390 mV [63,64], as determined by redox titrations. The redox potential has been observed to shift following different treatments to PSII, and it has been hypothesized that the shift in redox potential may play a functional role in decreasing photoinhibition *in vivo* [41]. Both the photooxidation and photoreduction (at higher light levels) of Cyt b_{559} have been observed [36,65]. The structure, spectroscopic properties, and electron-transfer reactions of Cyt b_{559} have been previously reviewed [19,25–27].

3.1. LP/HP interconversion

A conversion from HP to LP or IP Cyt b_{559} has been observed under a variety of conditions, including the removal of lipids [66], Tris washing [67–69], the removal of Car [70], heat treatment [69,71–73], salt washing [74,75], the removal of the 17- and 23-kDa extrinsic subunits [49,63], alkaline pH incubation [69], and high light illumination at 5000 μE/m^2s [76], perhaps due to the complete reduction of Q_A and Q_B [41]. However, the conversion from LP to HP Cyt b_{559} has proven to be more difficult to achieve experimentally, although it has been observed that the Cyt b_{559} present in the stromal membranes is mainly in the LP form, while the HP form is enriched in the appressed regions, indicating that a conversion process takes place *in vivo* [77]. Experimentally, a 50–60% restoration of HP Cyt b_{559} has been achieved by the addition of PQ to heptane-extracted chloroplasts [70]. The incorporation of PSII core complexes, which contain only LP Cyt b_{559}, into liposomes composed of digalactosyldiacylglycerol and phosphatidylcholine resulted in a conversion of a portion of the LP Cyt b_{559} into the HP form (as defined by reducibility by 20 mM hydroquinone), while a slightly greater portion remained in the LP form [78]. In Mn-depleted PSII samples, it was observed that reducing conditions and anaerobicity resulted in the conversion of 60% of Cyt b_{559} into the HP form, which was reversible upon the addition of oxygen, and the conversion was absent in O_2-evolving PSII samples [79]. It has been hypothesized that binding of PQ at a site near Q_B may increase the redox potential of HP Cyt b_{559} [80,81]. However, despite extensive study, a method for reversibly converting 100% of Cyt b_{559} from the HP to LP form has not been discovered, and the structural and functional differences between the HP, IP, and LP forms have not been identified. It is likely that the differences in redox potential are due to the protein environment surrounding the heme, and not to changes in the ligation of the His residues, based on the similar EPR spectra observed for the different forms [63] and the structural similarity of the LP heme to model complexes [82]; however, it has also been observed that the HP form has a different absorbance signature in the Soret region of the visible spectrum [64]. Well-defined structural characterization of the different forms of Cyt b_{559}, and methods for their interconversion, will yield insight on the functional role of each form.

3.2. Site-directed mutagenesis on Cyt b_{559}

Although many mutations to Cyt b_{559} prevent the assembly of PSII, some site-directed mutants have been successfully isolated. Site-directed mutation of the heme-binding His23 ligand from the α subunit to Tyr or Met yielded PSII complexes that lacked the heme of Cyt b_{559}, either due to its total absence from the complex or to loss during isolation of PSII, and were as capable of oxygen evolution as WT, but more sensitive to photodamage [83]. The mutation in the β subunit of Phe26, about 15 Å away from the Fe approximately in the plane of the heme, to Ser resulted in PSII that retained a reduced PQ pool in the dark. In contrast, the PQ pool of WT PSII undergoes reoxidation in the dark [84,85], which suggests that Cyt b_{559} may be involved in the oxidation of

the PQ pool in the dark [86,87]. A mutation to the axial heme ligand in the α subunit, His22Lys [88], and mutation of a residue near the heme, Tyr18Ser, resulted in mainly LP Cyt b_{559} and increased photoinhibition compared to WT, attributed to a change in ligation of the heme and to a change in hydrophobicity near the heme, respectively [89]. The Arg7Leu mutation, nearby the heme, resulted in heme ligand displacement and enhanced photoinhibition [90]. LP Cyt b_{559} was also formed in cells with a deletion in the gene for the Psb30 protein, and photoinhibition was again increased [91]. Overall, the characterization of PSII containing mutations in Cyt b_{559} indicates that Cyt b_{559} plays a role in both the structure of PSII and in photoprotection of the protein.

4. Structure

4.1. Structure of each cofactor

Resonance Raman, high-field EPR, ESEEM, and HYSCORE spectroscopies have provided structural information about the individual cofactors involved in secondary electron transfer within PSII. The conformation of the cofactors affects their redox potentials as well as the edge-to-edge distance for electron transfer. Resonance Raman spectroscopy has shown that the redox-active carotenoids in *Synechocystis* PSII are in an all-*trans* configuration [57,92–94]. High-field EPR spectroscopy has been used to separately resolve the signals from $Car^{\bullet+}$ and $Chl^{\bullet+}$, indicating that the structure of $Car^{\bullet+}$ is similar to a canthaxanthin radical with a slightly rhombic tensor, while $Chl^{\bullet+}$ is similar to monomeric $Chl^{\bullet+}$ in methylene chloride [60,95]. Pulsed ^{1}H ENDOR spectroscopy has indicated that the $Car^{\bullet+}$ in PSII are as symmetrical as $Car^{\bullet+}$ *in vitro*, with the radical delocalized along the polyene chain [96]. This interpretation is also supported by high-field EPR [97], resonance Raman spectroscopy [98], and density functional theory (DFT) calculations [99].

By comparison to the selectively ^{15}N-labelled model complex Fe(III)–protoporphyrin IX $(Im)_2$, it was determined that the structure of the heme in LP Cyt b_{559} is very similar to that of the model complex, with the unpaired electron in a non-bonding iron orbital [82]. Overall, it seems that the cofactors in PSII are in similar conformations as the compounds dissolved in solution; therefore, any unusual redox properties are most likely due to their protein surroundings, including the unusually high and variable redox potential of Cyt b_{559}.

4.2. Location of each cofactor

4.2.1. Spectroscopic measurements

Higher resolution crystal structures have shown the location and arrangement of each cofactor (see Section 4.2.2). However, there has been some difficulty in localizing or distinguishing each component, most notably Car, which has an appearance similar to a phytol tail of Chl, Pheo, or PQ. In addition, crystallography cannot identify which Chl and Car molecules are redox active. Hence, other spectroscopic techniques have been used to determine the locations of specific redox cofactors with respect to others. The spin-lattice relaxation rates calculated from pulsed high-frequency EPR spectroscopy indicated that on average $Car^{\bullet+}$ is 38 ± 1 Å from the non-heme iron, and the average $Chl^{\bullet+}$ is ≥ 40 Å from the non-heme iron [100]. Consistent with those values, X-band saturation-recovery EPR experiments have shown that the weighted average of $Car^{\bullet+}$ and $Chl^{\bullet+}$ is 39 ± 2.5 Å from the non-heme iron [101]. Pulsed EPR spectroscopy has shown that the OEC, Q_A, and $Chl^{\bullet+}$ are 27 Å [102], 38.5 Å, and 29.4 Å from Y_D [103,104], respectively, while Y_Z and Y_D are both 37 ± 5 Å from the non-heme iron [105].

Relative orientations of the redox-active cofactors have also been determined. Pulsed EPR spectroscopy experiments have yielded the angular relationship between Y_Z, Y_D, and the OEC [106], and the vector between Y_D and $Chl^{\bullet+}$ and the membrane normal has been found to be $50 \pm 5°$ based on a distance of 29.5 Å between Y_Z and Y_D [107,108]. By HYSCORE spectroscopy, it has been shown that one indole nitrogen from a tryptophan residue interacts with $Car^{\bullet+}$ [109]. $Chl^{\bullet+}$ species, generated by illumination at 198 K, on average have ring planes oriented perpendicular to the membrane plane based on high-frequency EPR [61], and two spectrally-separable Car species have been observed by linear dichroism of PSII core complexes with one oriented parallel to the membrane plane and one tilted approximately 45° [110,111].

Based on computational structural analysis [112], rates of energy transfer observed by transient absorption difference spectroscopy [113], absorbance spectroscopy [114], and electrochromic difference spectroscopy [115], it was proposed that D1-His118 and D2-His117 were the ligands to the accessory Chls closest to P_{680}. This was supported by disrupted exciton transfer in site-directed mutants of D2-His117 and D1-His118 [116–118] and by the characteristic growth of the mutants [119,120]. Based on saturation-recovery EPR spectroscopy and homology to the bacterial reaction center, it was further proposed that D1-His118 and D2-His117 were ligands to the redox-active Chls named "$Chl_Z^{\bullet+}$" [101]. This hypothesis was confirmed by perturbed resonance Raman spectra of a Mn-depleted D1-H118Q *Synechocystis* PSII sample [121] following selective excitation into the 820 nm absorbance band of $Chl^{\bullet+}$ [56]. Interestingly, the EPR and near-IR spectra of the mutant were similar to those of wild type [121]. $Chl^{\bullet+}$ has been observed to quench fluorescence [54], and mutational studies of D1-His118 ligated to Chl_{ZD1} (historically known as Chl_Z) and D2-His117 ligated to Chl_{ZD2} (historically known as Chl_D) indicated that mutations around Chl_{ZD2} decreased the amount of fluorescence quenching in cyanobacteria [122,123]. In contrast, FTIR spectroscopy has indicated that both Chl_{ZD1} and Chl_{ZD2} may be photooxidized in higher plants [124]. The location of $Chl^{\bullet+}$ remains uncertain, and may have variability between species.

4.2.2. X-ray crystallography

Low-resolution cryo-electron microscopy has shown the general structure and trans-membrane helix positions in PSII [125–130], while recent X-ray crystallography [40,131–140] studies have provided a clear picture of the overall structure of PSII and the locations of all of the cofactors; however these structural methods cannot identify which of the Chl and Car cofactors are redox-active and involved in secondary electron transfer. As shown in Figs. 1A and 2, Car_{D2} is the closest secondary donor to P_{680}, and it is likely that this Car is the initial secondary donor, which is also consistent with spectroscopic studies [58]. Shown in Fig. 2, once Car_{D2} has been oxidized, there are many adjacent cofactors that may be involved in secondary electron transfer. These include Chl_{ZD2}, Cyt b_{559}, and other Car and Chl cofactors. Hence, it is possible that an oxidizing equivalent on Car_{D2} could be transferred to a wide selection of the closely spaced 35 Chl and 11 Car molecules per PSII when Cyt b_{559} is preoxidized.

Carotenoids are found in the periphery of PSII cores, spanning the membrane, with many subunits involved in Car binding. Chlorophylls are clustered together primarily in CP43 and CP47, with some in close proximity to Car [141]. Distances between cofactors, indicated in Fig. 2, include 11.1 Å from B_B to Car_{D2} and 11.6 Å from to Car_{D2} to Cyt b_{559}. These short distances provide an efficient pathway for electron transfer from P_{680} to Cyt b_{559} via Car_{D2}. From Car_{D2}, Chl_{ZD2} is 4.9 Å away, which is in turn 14.4 Å away from a Chl molecule in close proximity to the other Chl/Car cofactors in CP47. Car_{D2} is also 10.7 Å away from another Car in close proximity to the other Chl/Car cofactors in CP43, one of which is 15.4 Å from Chl_{ZD1}. Within CP43 and CP47, the distances between Chl/Car cofactors range from less than 4 Å to around 8 Å, with almost all distances less than 6 Å. The redox potentials of $Car^{\bullet+}$ and $Chl^{\bullet+}$ are relatively similar [142] and the Chl/Car cofactors are arranged with short distances for single electron-transfer steps; therefore, the radical hole may quickly equilibrate throughout the Chl/Car cofactors, possibly into CP43 and CP47, as shown in Fig. 2.

From the 1.9 Å resolution crystal structure [40], the redox-active Car in D2 is approximately parallel to the membrane plane, 11 Å from Cyt b_{559}, 5.0 Å from Chl_{ZD2}, 11 Å from another Car, and passes within 10 Å of

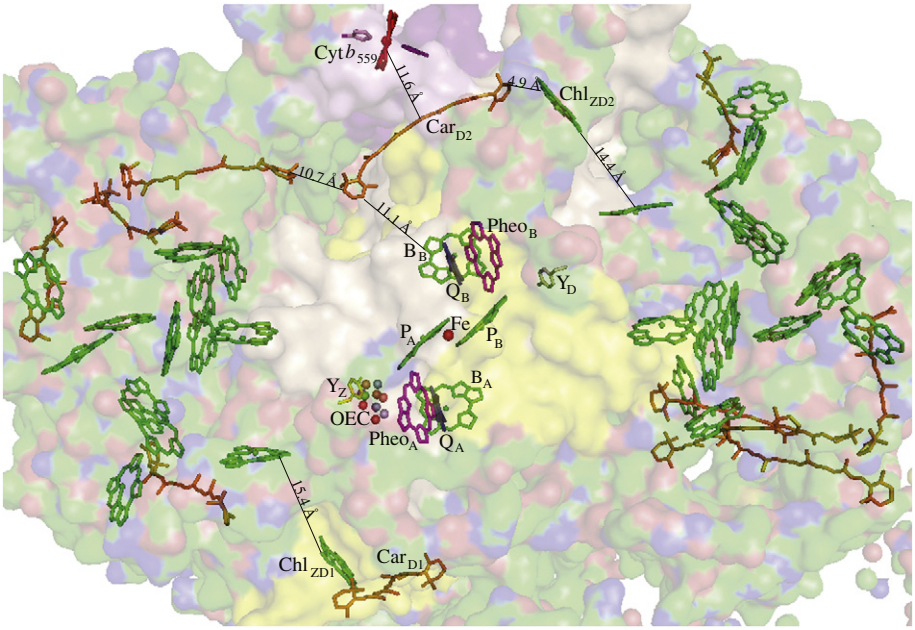

Fig. 2. The arrangement of cofactors in PSII, viewed from the membrane surface (PDB ID: 3ARC). The oxygen-evolving complex (OEC) is shown with manganese atoms in purple, oxygen in red, and calcium in green; tyrosine Z (Y_Z) is shown in yellow and tyrosine D (Y_D) is shown in tan; chlorophylls (Chl) are shown in green; β-carotene (Car) is shown in orange; pheophytins ($Pheo_A$ and $Pheo_B$) are shown in magenta; and quinones (Q_A and Q_B) are shown in blue. The surfaces of the D1, D2, α- and β-Cyt b_{559} subunits are colored yellow, tan, pink and purple, respectively, with the remaining surfaces colored according to atom identity. The longest distances (in Å) between neighboring cofactors are shown as solid lines, with the unlabelled distances being mainly less than 6 Å.

the tails of Q_B an B_B. Car_{D2} is 28 Å from the non-heme iron, which is shorter than the average 38 Å observed by saturation recovery EPR [100], indicating that the other $Car^{\bullet+}$ (see Section 5) is further from the non-heme iron, perhaps in CP43 or CP47. Chl_{ZD2}, in addition to the proximity to Car_{D2}, is approximately 14 Å from a Chl in CP47, in which the cofactors are very closely spaced, and 6.0 Å from the tail of Q_B. Car_{D1} is approximately perpendicular to the membrane plane, 5 Å from Chl_{ZD1}, 13 Å from the tails of Q_A, Pheo, and B_A, and 35 Å from the non-heme iron. Chl_{ZD1} is approximately 16 Å from both Chl and Car in CP43. The cofactors in CP43 and CP47 are bridged by Chl_{ZD2}, 14 Å from CP47, through Car_{D2} and its adjoining Car 11 Å away, which is 3.9 Å from the cofactors grouped in CP43. Several negatively charged lipids are located near Chl in CP43 (4.3 Å away) and CP47 (5.3 Å away), which have been hypothesized to decrease the redox potential of Chl, resulting in more stable radicals [143,144]. Negatively charged lipids are also located 5.5 Å away from a Car in CP47, and 6.1 Å away from Car_{D1}. The observation by HYSCORE that $Car^{\bullet+}$ is coupled to the N of a Trp is supported by the fact that Car_{D2} is 7.8 Å from a Trp residue [109]. Additionally, Trp residues are close to several other Car molecules, including 5.1 Å from a Car in CP43.

The heme of LP Cyt b_{559} is ligated by one His from the β-subunit of Cyt b_{559} (*psbF* gene product) at a distance of 2.15 Å, with the imidazole ring bisecting the N-Fe(III)-N angle, and one His from the α-subunit (*psbE* gene product) at 2.03 Å with the imidazole ring at an angle of approximately 22.5° to the other. The plane of the heme is slightly twisted.

4.2.2.1. Q_C site. The 2.9 Å resolution crystal structure has provided some evidence that binding of PQ to PSII may occur at a site other than Q_B in the hydrophobic cavity near Cyt b_{559} [138,144]. Binding of inhibitors has previously been observed at a site separate from Q_B, which could modulate the environment of the heme in Cyt b_{559}, its redox potential, and its electron-transfer properties [80,87]. However, occupancy of the Q_C site was not observed in the 1.9 Å resolution crystal structure [40], possibly due to higher disorder in the binding of PQ to the site [138] stemming from low affinity or non-specific binding, or to loss during preparation of the crystals.

4.2.2.2. Calculations from X-ray structures. A wide variety of spectroscopic properties may be calculated using distances from the X-ray structures in conjunction with quantum parameters. Possible energy transfer pathways [145] and the ability of $Chl^{\bullet+}$ to quench fluorescence [146] have been modeled and compared with experimental data. The redox potentials of Chl and Car have also been calculated based on crystal structures up to 3.0-Å resolution, and it has been found that the redox potential of Car and Chl in D1 are higher than those in D2, which may indicate a preference for radical localization in D2 [142,147], although these potentials may be modified by slight conformational changes in the protein. The calculation of CD and LD spectra, excitonic coupling, domain structure, site energies, and exciton transfer from structural data has been previously reviewed in Ref. [141].

5. Progress in characterization of secondary electron transfer

Following the identification of the redox-active secondary cofactors (see Section 2), it was shown that Cyt b_{559}, $Car^{\bullet+}$, and $Chl^{\bullet+}$ are members of the same secondary electron-transfer pathway. Most of the studies of the secondary electron-transfer reactions have been carried out by illuminating PSII at cryogenic temperatures, under which conditions PSII is limited to a single stable charge separation [30]. When Cyt b_{559} is prereduced, it is the preferential (lowest potential) electron donor at cryogenic temperatures. Its quantitative photooxidation upon illumination, to generate the Cyt b_{559}^{ox} $Q_A^{\bullet-}$ charge separation, can be observed by EPR [30] and optical spectroscopy [8]. However, low-temperature illumination of a PSII sample in which Cyt b_{559} is preoxidized generates a distribution of $Chl^{\bullet+}$ $Q_A^{\bullet-}$ and $Car^{\bullet+}$ $Q_A^{\bullet-}$ charge-separated states. In contrast, Y_D oxidation is on a separate pathway, which increasingly competes with the secondary electron-transfer pathway at higher pH [148].

Although the side-path donors do not operate at a high efficiency, organisms with enhanced cyclic electron transfer have been observed to be more resistant to photodamage [149,150]. Additionally, at 77 K, the Cyt b_{559}^{ox}/Q_A^- charge separation can be generated in almost 100% of PSII centers with pre-reduced Cyt b_{559} [8]. At room temperature, the yield of oxidized Cyt b_{559} in PSII-enriched membranes inactive for O_2 evolution

following a single flash was approximately double (4.7%) the yield in an O_2-evolving sample, and the maximum yield of oxidized Cyt b_{559} was reached after 21 s of continuous illumination in an O_2-evolving sample, compared to 1.8 s for an inactive sample [36]. Due to the highly-oxidizing nature of $P_{680}^{\bullet+}$, the secondary donors, including the initial donor Car_{D2}, must be partially spatially separated from P_{680} so that their oxidation does not compete with water oxidation at the OEC under physiological conditions [24]. However, they may play a photoprotective role in low yield when the lifetime of $P_{680}^{\bullet+}$ is long.

Species differences in the secondary electron-transfer pathway have been noticed between higher plants and cyanobacteria. For example, at high pH, $Y_D^{\bullet}$ was formed in 75% of PSII centers in *Synechocystis* and 55% of centers in spinach [148]. The rate of $P_{680}^{\bullet+}/Q_A^-$ recombination is slower in cyanobacterial PSII than in higher plant PSII [1,5]. The yield and identity of $Chl^{\bullet+}$ have also been observed to vary between plant and cyanobacterial PSII [20]. These differences may reflect differential mechanisms of photoprotection, such as the addition of the xanthophyll cycle in higher plants, or changes in auxiliary proteins since the divergence of photosynthetic eukaryotes and cyanobacteria [151].

Although electron transfer is known to occur among Cyt b_{559}, $Car^{\bullet+}$, and $Chl^{\bullet+}$, the sequence of events and electron-transfer partners are not well defined. The rate of electron transfer depends on the distance between cofactors, the difference in redox potentials, and on the reorganization energy required [152]. The distribution of $Chl^{\bullet+}$ $Q_A^{\bullet-}$ and $Car^{\bullet+}$ $Q_A^{\bullet-}$ charge-separated states generated at low temperature has been interpreted to arise from the trapping of a distribution of conformations of PSII that have slightly different redox potentials of the Chl and Car cofactors when a sample of PSII is frozen [20]. Because Chl and Car generally have similar redox potentials, for a given conformation of PSII, either one of the Chl or one of the Car species will have the lowest redox potential and become the final electron donor when an oxidizing equivalent equilibrates among the secondary Chl/Car electron donors. Using the 3.7 Å resolution crystal structure [132], an electron-transfer pathway from P_{680} to Car_{D2} to Chl_{ZD1} was proposed involving a series of Chls in CP43 [146]. Although many electron transfer steps are required to reach Chl_{ZD1}, an electron will tunnel to any redox center with the correct midpoint potential, whenever the distance through other cofactors is short enough, even if an individual step is unfavorable [152].

Different PSII preparations, containing a variable number of subunits, may result in different solvent exposure and hence redox potentials for the cofactors. A PSII reaction center complex, containing only D1/D2/Cyt b_{559}, has the highest solvent exposure, whereas PSII core complexes, lacking the LHC-II proteins, have an intermediate amount of solvent exposure compared to PSII-enriched membranes or chloroplasts. These differences may explain, in part, differences in the secondary electron-transfer reactions in these different types of PSII preparations.

Near-IR spectroscopy has been a valuable tool for elucidating the relationships between the secondary donors under a variety of conditions. The near-IR spectrum of PSII (Fig. 3) exhibits the strong $D_0 \rightarrow D_2$ transition of $Car^{\bullet+}$ near 990 nm with an extinction coefficient of 160,000 M^{-1} cm^{-1} [153]. $Chl^{\bullet+}$ has a weaker absorbance at 800 to 850 nm with an extinction coefficient of 7000 M^{-1} cm^{-1} [154]. In addition, an absorbance at 750 nm is attributed to a neutral β-carotene radical ($Car^{\bullet}$) [155]. Recently, an absorbance at 1450 nm attributed to the $D_0 \rightarrow D_1$ transition of $Car^{\bullet+}$ has also been observed [156].

5.1. Properties of secondary electron transfer in PSII with mostly LP/IP Cyt b_{559}

5.1.1. Higher plant PSII containing LP/IP Cyt b_{559}

In active, O_2-evolving samples, Cyt b_{559} is mostly in the HP and IP form [63,64], and predominantly reduced under ambient conditions, while inactive, non-O_2-evolving samples contain the IP and LP forms, which are typically oxidized under ambient conditions. In a study of inactive PSII reaction center complexes (D1/D2/Cyt b_{559}) from spinach, it was observed by resonance Raman spectroscopy that two Car molecules were photooxidized, one more easily than the other, and at least three Chl molecules were also photooxidized [93]. These results supported work done on inactive PSII reaction center complexes (D1/D2/Cyt b_{559}) from pea plants [157]. By near-IR spectroscopy on PSII-enriched membranes, two $Chl^{\bullet+}$ bands were observed, attributed to $Chl_{ZD1}^{\bullet+}$ ("$Chl_Z^{\bullet+}$") and $Chl_{ZD2}^{\bullet+}$ ("$Chl_D^{\bullet+}$") and it was observed that $Car^{\bullet+}$ decayed mainly by recombination with $Q_A^{\bullet-}$, but also partly by the formation of $Chl^{\bullet+}$ absorbing at 850 nm [20].

5.1.2. Cyanobacterial PSII containing LP/IP Cyt b_{559}

In non-O_2 evolving, inactive *Synechocystis* PSII samples, one $Chl^{\bullet+}$ peak was observed by near-IR spectroscopy, in contrast to two $Chl^{\bullet+}$ peaks observed in inactive spinach PSII samples, and it was attributed to $Chl_{ZD1}^{\bullet+}$ ("$Chl_Z^{\bullet+}$") [20,143]. The $Car^{\bullet+}$ peak in inactive *Synechocystis* PSII samples was observed to shift as the radical decayed, indicating the presence of two redox-active Car absorbing at 982 and 1027 nm that were affected differently by the presence of $Y_D^{\bullet}$ in the sample [143,158]. $Car^{\bullet+}$ in these samples decayed only by recombination with $Q_A^{\bullet-}$ and not by conversion to $Chl^{\bullet+}$, and $Car^{\bullet+}$ decayed more rapidly than $Chl^{\bullet+}$ by recombination with $Q_A^{\bullet-}$, indicating its closer proximity to Q_A [20].

Illumination of PSII samples with a mixture of oxidized LP Cyt b_{559} and reduced HP Cyt b_{559} results in the formation of $Car^{\bullet+}$ and $Chl^{\bullet+}$ in the PSII centers with LP Cyt b_{559}, whereas Cyt b_{559} oxidation occurred in the remainder of the centers. In PSII samples with oxidized LP Cyt b_{559}, the peak from $Car^{\bullet}$, which may be involved in fluorescence quenching, was not observed at 750 nm, and the wavelength maximum of the $Car^{\bullet+}$ peak was shifted to the red compared to centers containing oxidized IP and HP Cyt b_{559}. These changes indicate that different Chl and Car cofactors are oxidized in centers containing different redox forms of Cyt b_{559}, implying different pathways and/or outcomes of secondary electron transfer in response to shifts in the midpoint potential of Cyt b_{559} [159].

5.2. Properties of secondary electron transfer in PSII with mostly HP Cyt b_{559}

5.2.1. Higher plant PSII containing HP/IP Cyt b_{559}

In samples of O_2-evolving PSII-enriched membranes solubilized with 0.5% β-DM, near-IR spectroscopy showed that the $Car^{\bullet+}$ peak had a wavelength maximum around 1010 nm. Compared to non-O_2-evolving, inactive spinach samples of PSII-enriched membranes, the $t_{1/2}$ for the formation of $Car^{\bullet+}$ absorbing at 970 nm was similar to that in the O_2-evolving samples, but more $Chl^{\bullet+}$ absorbing at 820 nm remained after a series of flashes, implying an altered secondary electron transfer pathway between active and inactive spinach PSII centers [160].

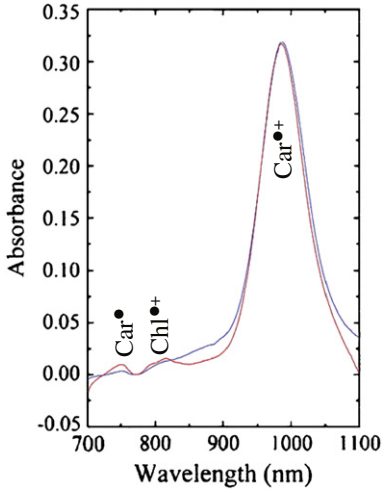

Fig. 3. Light-minus-dark difference spectra of Mn-depleted *Synechocystis* PSII (blue) and O_2-evolving *Synechocystis* PSII (red); modified from Ref. [159].

5.2.2. Cyanobacterial PSII containing HP/IP Cyt b_{559}

In contrast to non-O_2-evolving, inactive cyanobacterial samples, O_2 evolving samples contained $Chl^{\bullet+}$ peaks with more structure and a narrower $Car^{\bullet+}$ peak, perhaps due to a more homogeneous protein structure in the presence of the OEC [143]. The $Car^{\bullet+}$ peak again contained contributions from two different $Car^{\bullet+}$ cofactors absorbing maximally at 984 and 1029 nm; however, the $Chl^{\bullet+}$ peaks contained contributions from five spectrally distinct $Chl^{\bullet+}$ cofactors, rather than one or two, which formed and decayed at different rates. The amount of some $Chl^{\bullet+}$ species continued to increase after total charge separation had been achieved, indicating conversion among the different $Chl^{\bullet+}$, and also perhaps between the $Car^{\bullet+}$, with the most stable $Chl^{\bullet+}$ absorbing at 810 nm [143].

5.3. Properties of secondary electron transfer in PSII with modified pigments

A portion of the pigments in PSII complexes may be removed by washing with Triton-X 100 [161] or using Cu-immobilized chromatography [162]. It has been observed in these systems that Car is capable of quenching $^1O_2$ [161], and that secondary electron transfer is possible in the D1 subunit [162] at room temperature [163]. Site-directed mutagenesis of D1-Thr179, nearby to Chl B_A, indicated that the presence of $Car_{D2}^{\bullet+}$, $Chl_{ZD2}^{\bullet+}$, and Q_A^- resulted in a blue shift of the Chl B_A Q_Y absorbance band [164].

PSII will not assemble without Chl [119,120] or Car [165], which indicates a structural requirement for the cofactors. However, genetic manipulation of the carotenoid biosynthesis genes in *Synechocystis* resulted in the growth of cells containing β-zeacarotene, with 9 conjugated double bonds and only one β-ionylidene ring, instead of β-carotene, which contains 11 conjugated double bonds and two β-ionylidene rings [165]. PSII isolated from these cells displayed a $Car^{\bullet+}$ absorbance maximum at 898 nm and a higher ratio of $Chl^{\bullet+}/Car^{\bullet+}$, both consistent with the shorter conjugation length and higher redox potential of β-zeacarotene.

6. Summary

The photooxidation of the secondary electron donors, Cyt b_{559}, Car, and Chl, has been observed in PSII under a variety of conditions. Although the yield of photooxidized secondary donors is low under physiological conditions, they are believed to play a photoprotective role when electron transfer resulting in water-oxidation catalysis is inhibited. Cyt b_{559}, with LP, IP, and HP forms, is preferentially oxidized by $P_{680}^{\bullet+}$ through a network of Car and Chl cofactors. Cyt b_{559} may also be reduced by the acceptor side of PSII, thereby forming a cyclic electron-transfer pathway that connects the donor and acceptor sides of PSII to remove potentially harmful, excess oxidizing equivalents. The structure of Cyt b_{559} has been characterized by X-ray crystallography, but the structural differences between the LP, IP and HP forms of Cyt b_{559} remain to be determined, as does the physiological role for their conversion. The structure and arrangement of Car and Chl cofactors have also been determined by X-ray crystallography, and their redox activity has been probed by a variety of spectroscopic methods. Electron transfer among the secondary donors involves many Car and Chl cofactors, especially in O_2-evolving samples, which appear to be connected in a network extending into the peripheral subunits of PSII (CP43 and CP47), rather than involving only a few cofactors in a simple pathway. The sequence of electron-transfer steps and the location of each redox-active Car and Chl cofactor, however, remain to be determined.

References

[1] R. de Wijn, H.J. van Gorkom, The rate of charge recombination in photosystem II, Biochim. Biophys. Acta Bioenerg. 1553 (2002) 302–308.
[2] S. Reinman, P. Mathis, H. Conjeaud, A. Stewart, Kinetics of reduction of the primary donor of photosystem II. Influence of pH in various preparations, Biochim. Biophys. Acta Bioenerg. 635 (1981) 429–433.
[3] H. Conjeaud, P. Mathis, The effect of pH on the reduction kinetics of P-680 in tris-treated chloroplasts, Biochim. Biophys. Acta Bioenerg. 590 (1980) 353–359.
[4] J. Haveman, P. Mathis, Flash-induced absorption changes of the primary donor of photosystem II at 820 nm in chloroplasts inhibited by low pH or tris-treatment, Biochim. Biophys. Acta Bioenerg. 440 (1976) 346–355.
[5] J.G. Metz, P.J. Nixon, M. Rögner, G.W. Brudvig, B.A. Diner, Directed alteration of the D1 polypeptide of photosystem II: evidence that tyrosine-161 is the redox component, Z, connecting the oxygen-evolving complex to the primary electron donor, P_{680}, Biochemistry 28 (1989) 6960–6969.
[6] S. Gerken, J.P. Dekker, E. Schlodder, H.T. Witt, Studies on the multiphasic charge recombination between chlorophyll a_{II}^+ (P-680$^+$) and plastoquinone Q_A^- in photosystem II complexes. Ultraviolet difference spectrum of Chl-a_{II}^+/Chl-a_{II}, Biochim. Biophys. Acta Bioenerg. 977 (1989) 52–61.
[7] C.A. Buser, L.K. Thompson, B.A. Diner, G.W. Brudvig, Electron-transfer reactions in manganese-depleted photosystem II, Biochemistry 29 (1990) 8977–8985.
[8] B. Hillmann, E. Schlodder, Electron transfer reactions in photosystem II core complexes from *Synechococcus* at low temperature — difference spectrum of P_{680}^+ Q_A^-/P_{680} Q_A at 77 K, Biochim. Biophys. Acta Bioenerg. 1231 (1995) 76–88.
[9] B.A. Diner, D.A. Force, D.W. Randall, R.D. Britt, Hydrogen bonding, solvent exchange, and coupled proton and electron transfer in the oxidation and reduction of redox-active tyrosine Y_Z in Mn-depleted core complexes of photosystem II, Biochemistry 37 (1998) 17931–17943.
[10] B.A. Diner, F. Rappaport, Structure, dynamics, and energetics of the primary photochemistry of photosystem II of oxygenic photosynthesis, Annu. Rev. Plant Biol. 53 (2002) 551–580.
[11] M. Grabolle, H. Dau, Energetics of primary and secondary electron transfer in photosystem II membrane particles of spinach revisited on basis of recombination-fluorescence measurements, Biochim. Biophys. Acta Bioenerg. 1708 (2005) 209–218.
[12] F. Rappaport, M. Guergova-Kuras, P.J. Nixon, B.A. Diner, J. Lavergne, Kinetics and pathways of charge recombination in photosystem II, Biochemistry 41 (2002) 8518–8527.
[13] Z. Li, S. Wakao, B.B. Fischer, K.K. Niyogi, Sensing and responding to excess light, Annu. Rev. Plant Biol. 60 (2009) 239–260.
[14] J.R. Durrant, L.B. Giorgi, J. Barber, D.R. Klug, G. Porter, Characterisation of triplet states in isolated photosystem II reaction centres: oxygen quenching as a mechanism for photodamage, Biochim. Biophys. Acta Bioenerg. 1017 (1990) 167–175.
[15] I. Vass, S. Styring, Spectroscopic characterization of triplet forming states in photosystem II, Biochemistry 31 (1992) 5957–5963.
[16] A.N. Macpherson, A. Telfer, J. Barber, T.G. Truscott, Direct detection of singlet oxygen from isolated photosystem II reaction centres, Biochim. Biophys. Acta Bioenerg. 1143 (1993) 301–309.
[17] É. Hideg, C. Spetea, I. Vass, Singlet oxygen production in thylakoid membranes during photoinhibition as detected by EPR spectroscopy, Photosynth. Res. 39 (1994) 191–199.
[18] C. Fufezan, A.W. Rutherford, A. Krieger-Liszkay, Singlet oxygen production in herbicide-treated photosystem II, FEBS Lett. 532 (2002) 407–410.
[19] D.H. Stewart, G.W. Brudvig, Cytochrome b_{559} of photosystem II, Biochim. Biophys. Acta Bioenerg. 1367 (1998) 63–87.
[20] C.A. Tracewell, A. Cua, D.H. Stewart, D.F. Bocian, G.W. Brudvig, Characterization of carotenoid and chlorophyll photooxidation in photosystem II, Biochemistry 40 (2001) 193–203.
[21] P. Faller, C. Fufezan, A.W. Rutherford, Side-path electron donors: cytochrome b_{559}, chlorophyll Z and β-carotene, in: T.J. Wydrzynski, K. Satoh, J.A. Freeman (Eds.), Photosystem II: The Light-Driven Water:Plastoquinone Oxidoreductase, vol. 22, Springer, Dordrecht, The Netherlands, 2005, pp. 347–365.
[22] A. Telfer, What is β-carotene doing in the photosystem II reaction centre? Philos. Trans. R. Soc. Lond. B 357 (2002) 1431.
[23] C.A. Tracewell, J.S. Vrettos, J.A. Bautista, H.A. Frank, G.W. Brudvig, Carotenoid photooxidation in photosystem II, Arch. Biochem. Biophys. 385 (2001) 61–69.
[24] H.A. Frank, G.W. Brudvig, Redox functions of carotenoids in photosynthesis, Biochemistry 43 (2004) 8607–8615.
[25] A.-F. Miller, G.W. Brudvig, A guide to electron paramagnetic resonance spectroscopy of photosystem II membranes, Biochim. Biophys. Acta Bioenerg. 1056 (1991) 1–18.
[26] J. Whitmarsh, W.A. Cramer, A pathway for the reduction of cytochrome b_{559} by photosystem II in chloroplasts, Biochim. Biophys. Acta Bioenerg. 501 (1978) 83–93.
[27] W.A. Cramer, J. Whitmarsh, Photosynthetic cytochromes, Annu. Rev. Plant Biol. 28 (1977) 133–172.
[28] D.B. Knaff, D.I. Arnon, Light-induced oxidation of a chloroplast b-type cytochrome at -189 °C, Proc. Natl. Acad. Sci. U. S. A. 63 (1969) 956–962.
[29] A. Vermeglio, P. Mathis, Light-induced absorbance changes at −170 °C with spinach chloroplasts: charge separation and field effect, Biochim. Biophys. Acta Bioenerg. 368 (1974) 9–17.
[30] J.C. de Paula, J.B. Innes, G.W. Brudvig, Electron transfer in photosystem II at cryogenic temperatures, Biochemistry 24 (1985) 8114–8120.
[31] J. Whitmarsh, W.A. Cramer, Kinetics of the photoreduction of cytochrome b_{559} by photosystem II in chloroplasts, Biochim. Biophys. Acta Bioenerg. 460 (1977) 280–289.
[32] U. Heber, M.R. Kirk, N.K. Boardman, Photoreactions of cytochrome b_{559} and cyclic electron flow in photosystem II of intact chloroplasts, Biochim. Biophys. Acta Bioenerg. 546 (1979) 292–306.
[33] L.K. Thompson, G.W. Brudvig, Cytochrome b_{559} may function to protect photosystem II from photoinhibition, Biochemistry 27 (1988) 6653–6658.

[34] P.G. Falkowski, Y. Fujita, A. Ley, D. Mauzerall, Evidence for cyclic electron flow around photosystem II in *Chlorella pyrenoidosa*, Plant Physiol. 81 (1986) 310–312.
[35] O. Canaani, M. Havaux, Evidence for a biological role in photosynthesis for cytochrome b_{559} — a component of photosystem II reaction center, Proc. Natl. Acad. Sci. U. S. A. 87 (1990) 9295–9299.
[36] C.A. Buser, B.A. Diner, G.W. Brudvig, Photooxidation of cytochrome b_{559} in oxygen-evolving photosystem II, Biochemistry 31 (1992) 11449–11459.
[37] L. Nedbal, G. Samson, J. Whitmarsh, Redox state of a one-electron component controls the rate of photoinhibition of photosystem II, Proc. Natl. Acad. Sci. U. S. A. 89 (1992) 7929–7933.
[38] J. Whitmarsh, G. Samson, M. Poulson, Photoprotection in photosystem II — the role of cytochrome b_{559}, in: N.R. Baker, J.R. Bowyer (Eds.), Photoinhibition of Photosynthesis, Bios Scientific Publishers, Oxford, UK, 1994, pp. 75–93.
[39] M. Poulson, G. Samson, J. Whitmarsh, Evidence that cytochrome b_{559} protects photosystem II against photoinhibition, Biochemistry 34 (1995) 10932–10938.
[40] Y. Umena, K. Kawakami, J.-R. Shen, N. Kamiya, Crystal structure of oxygen-evolving photosystem II at a resolution of 1.9 Å, Nature 473 (2011) 55–60.
[41] J. Barber, J. De Las Rivas, A functional model for the role of cytochrome b_{559} in the protection against donor and acceptor side photoinhibition, Proc. Natl. Acad. Sci. U. S. A. 90 (1993) 10942–10946.
[42] T.S. Mor, T. Hundal, I. Ohad, B. Andersson, The fate of cytochrome b_{559} during anaerobic photoinhibition and its recovery processes, Photosynth. Res. 53 (1997) 205–213.
[43] J. De Las Rivas, B. Andersson, J. Barber, Two sites of primary degradation of the D1-protein induced by acceptor or donor side photo-inhibition in photosystem II core complexes, FEBS Lett. 301 (1992) 246–252.
[44] K.J. Yamashita, K. Konishi, M. Itoh, K. Shibata, Photo-bleaching of carotenoids related to the electron transport in chloroplasts, Biochim. Biophys. Acta Bioenerg. 172 (1969) 511–524.
[45] J.W.M. Visser, C.P. Rijgersberg, P. Gast, Photooxidation of chlorophyll in spinach chloroplasts between 10 and 180 K, Biochim. Biophys. Acta Bioenerg. 460 (1977) 36–46.
[46] B.R. Velthuys, Carotenoid and cytochrome b_{559} reactions in photosystem II in the presence of tetraphenylboron, FEBS Lett. 126 (1981) 272–276.
[47] P. Mathis, A.W. Rutherford, Effect of phenolic herbicides on the oxygen-evolving side of photosystem II. Formation of the carotenoid cation, Biochim. Biophys. Acta Bioenerg. 767 (1984) 217–222.
[48] C.C. Schenck, B. Diner, P. Mathis, K. Satoh, Flash-induced carotenoid radical cation formation in photosystem II, Biochim. Biophys. Acta Bioenerg. 680 (1982) 216–227.
[49] J.C. de Paula, P.M. Li, A.F. Miller, B.W. Wu, G.W. Brudvig, Effect of the 17- and 23-kilodalton polypeptides, calcium, and chloride and electron transfer in photosystem II, Biochemistry 25 (1986) 6487–6494.
[50] A. Telfer, J. De Las Rivas, J. Barber, β-Carotene within the isolated photosystem II reaction centre: photooxidation and irreversible bleaching of this chromophore by oxidised P680, Biochim. Biophys. Acta Bioenerg. 1060 (1991) 106–114.
[51] A. Telfer, W.-Z. He, J. Barber, Spectral resolution of more than one chlorophyll electron donor in the isolated photosystem II reaction centre complex, Biochim. Biophys. Acta Bioenerg. 1017 (1990) 143–151.
[52] T. Noguchi, T. Mitsuka, Y. Inoue, Fourier transform infrared spectrum of the radical cation of β-carotene photoinduced in photosystem II, FEBS Lett. 356 (1994) 179.
[53] S.E.J. Rigby, J.H.A. Nugent, P.J. O'Malley, ENDOR and special triple resonance studies of chlorophyll cation radicals in photosystem 2, Biochemistry 33 (1994) 10043–10050.
[54] R.H. Schweitzer, G.W. Brudvig, Fluorescence quenching by chlorophyll cations in photosystem II, Biochemistry 36 (1997) 11351–11359.
[55] A. Pascal, A. Telfer, J. Barber, B. Robert, Fourier-transform resonance Raman spectra of cation carotenoid in photosystem II reaction centres, FEBS Lett. 453 (1999) 11–14.
[56] A. Cua, D.H. Stewart, G.W. Brudvig, D.F. Bocian, Selective resonance Raman scattering from chlorophyll Z in photosystem II via excitation into the near-infrared absorption band of the cation, J. Am. Chem. Soc. 120 (1998) 4532–4533.
[57] J.S. Vrettos, D.H. Stewart, J.C. de Paula, G.W. Brudvig, Low-temperature optical and resonance Raman spectra of a carotenoid cation radical in photosystem II, J. Phys. Chem. B 103 (1999) 6403–6406.
[58] J. Hanley, Y. Deligiannakis, A. Pascal, P. Faller, A.W. Rutherford, Carotenoid oxidation in photosystem II, Biochemistry 38 (1999) 8189–8195.
[59] V.L. Tetenkin, B.A. Gulyaev, M. Seibert, A.B. Rubin, Spectral properties of stabilized D1/D2/cytochrome b_{559} photosystem II reaction center complex: effects of Triton X-100, the redox state of pheophytin, and β-carotene, FEBS Lett. 250 (1989) 459–463.
[60] K.V. Lakshmi, M.J. Reifler, G.W. Brudvig, O.G. Poluektov, A.M. Wagner, M.C. Thurnauer, High-field EPR study of carotenoid and chlorophyll cation radicals in photosystem II, J. Phys. Chem. B 104 (2000) 10445–10448.
[61] P. Faller, A.W. Rutherford, S. Un, High-field EPR study of carotenoid$^{\bullet+}$ and the angular orientation of chlorophyll $Z^{\bullet+}$ in photosystem II, J. Phys. Chem. B 104 (2000) 10960–10963.
[62] O. Nanba, K. Satoh, Isolation of a photosystem II reaction center consisting of D-1 and D-2 polypeptides and cytochrome b_{559}, Proc. Natl. Acad. Sci. U. S. A. 84 (1987) 109–112.
[63] L.K. Thompson, A.F. Miller, C.A. Buser, J.C. de Paula, G.W. Brudvig, Characterization of the multiple forms of cytochrome b_{559} in photosystem II, Biochemistry 28 (1989) 8048–8056.
[64] O. Kaminskaya, J. Kurreck, K.-D. Irrgang, G. Renger, V.A. Shuvalov, Redox and spectral properties of cytochrome b_{559} in different preparations of photosystem II, Biochemistry 38 (1999) 16223–16235.
[65] A. Magnuson, M. Rova, F. Mamedov, P.-O. Fredriksson, S. Styring, The role of cytochrome b_{559} and tyrosine$_D$ in protection against photoinhibition during *in vivo* photoactivation of photosystem II, Biochim. Biophys. Acta Bioenerg. 1411 (1999) 180–191.
[66] R.P. Cox, D.S. Bendall, The effects on cytochrome b_{559HP} and P_{546} of treatments that inhibit oxygen evolution by chloroplasts, Biochim. Biophys. Acta Bioenerg. 283 (1972) 124–135.
[67] K. Erixon, R. Lozier, W.L. Butler, The redox state of cytochrome b_{559} in spinach chloroplasts, Biochim. Biophys. Acta Bioenerg. 267 (1972) 375–382.
[68] D. Ghanotakis, C. Yocum, G. Babcock, ESR spectroscopy demonstrates that cytochrome b_{559} remains low potential in Ca^{2+}-reactivated, salt-washed PSII particles, Photosynth. Res. 9 (1986) 125–134.
[69] M. Roncel, A. Boussac, J. Zurita, H. Bottin, M. Sugiura, D. Kirilovsky, J. Ortega, Redox properties of the photosystem II cytochromes b_{559} and c_{550} in the cyanobacterium *Thermosynechococcus elongatus*, J. Biol. Inorg. Chem. 8 (2003) 206–216.
[70] R.P. Cox, D.S. Bendall, The functions of plastoquinone and β-carotene in photosystem II of chloroplasts, Biochim. Biophys. Acta Bioenerg. 347 (1974) 49–59.
[71] K. Wada, D.I. Arnon, Three forms of cytochrome b_{559} and their relation to the photosynthetic activity of chloroplasts, Proc. Natl. Acad. Sci. U. S. A. 68 (1971) 3064–3068.
[72] W.A. Cramer, J. Whitmarsh, P.S. Low, Differential scanning calorimetry of chloroplast membranes: identification of an endothermic transition associated with the water-splitting complex of photosystem II, Biochemistry 20 (1981) 157–162.
[73] L.K. Thompson, J.M. Sturtevant, G.W. Brudvig, Differential scanning calorimetric studies of photosystem II: evidence for a structural role for cytochrome b_{559} in the oxygen-evolving complex, Biochemistry 25 (1986) 6161–6169.
[74] J.-M. Briantais, C. Vernotte, M. Miyao, N. Murata, M. Picaud, Relationship between O_2 evolution capacity and cytochrome b_{559} high-potential form in photosystem II particles, Biochim. Biophys. Acta Bioenerg. 808 (1985) 348–351.
[75] D. Ghanotakis, C. Yocum, G. Babcock, ESR spectroscopy demonstrates that cytochrome b_{559} remains low potential in Ca^{2+}-reactivated, salt-washed PSII particles, Photosynth. Res. 9 (1986) 125–134.
[76] S. Styring, I. Virgin, A. Ehrenberg, B. Andersson, Strong light photoinhibition of electron transport in photosystem II. Impairment of the function of the first quinone acceptor, Q_A, Biochim. Biophys. Acta Bioenerg. 1015 (1990) 269–278.
[77] R.P. Cox, B. Andersson, Lateral and transverse organisation of cytochromes in the chloroplast thylakoid membrane, Biochem. Biophys. Res. Commun. 103 (1981) 1336–1342.
[78] H. Matsuda, W.L. Butler, Restoration of high-potential cytochrome b_{559} in photosystem II particles in liposomes, Biochim. Biophys. Acta Bioenerg. 725 (1983) 320–324.
[79] R. Gadjieva, F. Mamedov, G. Renger, S. Styring, Interconversion of low- and high-potential forms of cytochrome b_{559} in tris-washed photosystem II membranes under aerobic and anaerobic conditions, Biochemistry 38 (1999) 10578–10584.
[80] O. Kaminskaya, V.A. Shuvalov, G. Renger, Evidence for a novel quinone-binding site in the photosystem II (PS II) complex that regulates the redox potential of cytochrome b_{559}, Biochemistry 46 (2007) 1091–1105.
[81] O. Kaminskaya, V.A. Shuvalov, G. Renger, Two reaction pathways for transformation of high potential cytochrome b_{559} of PS II into the intermediate potential form, Biochim. Biophys. Acta Bioenerg. 1767 (2007) 550–558.
[82] I. García-Rubio, J.I. Martínez, R. Picorel, I. Yruela, P.J. Alonso, HYSCORE spectroscopy in the cytochrome b_{559} of the photosystem II reaction center, J. Am. Chem. Soc. 125 (2003) 15846–15854.
[83] F. Morais, K. Kühn, D.H. Stewart, J. Barber, G.W. Brudvig, P.J. Nixon, Photosynthetic water oxidation in cytochrome b_{559} mutants containing a disrupted heme-binding pocket, J. Biol. Chem. 276 (2001) 31986–31993.
[84] N. Bondarava, L. De Pascalis, S. Al-Babili, C. Goussias, J.R. Golecki, P. Beyer, R. Bock, A. Krieger-Liszkay, Evidence that cytochrome b_{559} mediates the oxidation of reduced plastoquinone in the dark, J. Biol. Chem. 278 (2003) 13554–13560.
[85] N. Bondarava, C.M. Gross, M. Mubarakshina, J.R. Golecki, G.N. Johnson, A. Krieger-Liszkay, Putative function of cytochrome b_{559} as a plastoquinol oxidase, Physiol. Plant. 138 (2010) 463–473.
[86] J. Kruk, K. Strzałka, Dark reoxidation of the plastoquinone-pool is mediated by the low-potential form of cytochrome b_{559} in spinach thylakoids, Photosynth. Res. 62 (1999) 273–279.
[87] J. Kruk, K. Strzalka, Redox changes of cytochrome b_{559} in the presence of plastoquinones, J. Biol. Chem. 276 (2001) 86–91.
[88] C.-H. Hung, J.-Y. Huang, Y.-F. Chiu, H.-A. Chu, Site-directed mutagenesis on the heme axial-ligands of cytochrome b_{559} in photosystem II by using cyanobacteria *Synechocystis* PCC 6803, Biochim. Biophys. Acta Bioenerg. 1767 (2007) 686–693.
[89] C.-H. Hung, H.J. Hwang, Y.-H. Chen, Y.-F. Chiu, S.-C. Ke, R.L. Burnap, H.-A. Chu, Spectroscopic and functional characterizations of cyanobacterium *Synechocystis* PCC 6803 mutants on and near the heme axial ligand of cytochrome b_{559} in photosystem II, J. Biol. Chem. 285 (2010) 5653–5663.
[90] Y.-F. Chiu, W.-C. Lin, C.-M. Wu, Y.-H. Chen, C.-H. Hung, S.-C. Ke, H.-A. Chu, Identification and characterization of a cytochrome b_{559} *Synechocystis* 6803 mutant spontaneously generated from DCMU-inhibited photoheterotrophical growth conditions, Biochim. Biophys. Acta Bioenerg. 1787 (2009) 1179–1188.
[91] M. Sugiura, S. Harada, T. Manabe, H. Hayashi, Y. Kashino, A. Boussac, Psb30 contributes to structurally stabilise the photosystem II complex in the thermophilic cyanobacterium *Thermosynechococcus elongatus*, Biochim. Biophys. Acta Bioenerg. 1797 (2010) 1546–1554.

[92] C.A. Tracewell, A. Cua, D.F. Bocian, G.W. Brudvig, Resonance Raman spectroscopy of carotenoids in photosystem II core complexes, Photosynth. Res. 83 (2005) 45–52.
[93] A. Telfer, D. Frolov, J. Barber, B. Robert, A. Pascal, Oxidation of the two β-carotene molecules in the photosystem II reaction center, Biochemistry 42 (2003) 1008–1015.
[94] M. Germano, A. Pascal, A.Y. Shkuropatov, B. Robert, A.J. Hoff, H.J. van Gorkom, Pheophytin-protein interactions in photosystem II studied by resonance Raman spectroscopy of modified reaction centers, Biochemistry 41 (2002) 11449–11455.
[95] P.J. Bratt, O. Poluektov, M.C. Thurnauer, J. Krzystek, L.C. Brunel, J. Schrier, Y.W. Hsiao, M. Zerner, A. Angerhofer, The g-factor anisotropy of plant chlorophyll $a^{\bullet+}$, J. Phys. Chem. B 104 (2000) 6973–6977.
[96] P. Faller, T. Maly, A.W. Rutherford, F. MacMillan, Chlorophyll and carotenoid radicals in photosystem II studied by pulsed ENDOR, Biochemistry 40 (2001) 320–326.
[97] T.A. Konovalova, J. Krzystek, P.J. Bratt, J. van Tol, L.-C. Brunel, L.D. Kispert, 95–670 GHz EPR studies of canthaxanthin radical cation stabilized on a silica–alumina surface, J. Phys. Chem. B 103 (1999) 5782–5786.
[98] A.S. Jeevarajan, L.D. Kispert, G. Chumanov, C. Zhou, T.M. Cotton, Resonance Raman study of carotenoid cation radicals, Chem. Phys. Lett. 259 (1996) 515–522.
[99] F. Himo, Density functional theory study of the β-carotene radical cation, J. Phys. Chem. A 105 (2001) 7933–7937.
[100] K.V. Lakshmi, O.G. Poluektov, M.J. Reifler, A.M. Wagner, M.C. Thurnauer, G.W. Brudvig, Pulsed high-frequency EPR study on the location of carotenoid and chlorophyll cation radicals in photosystem II, J. Am. Chem. Soc. 125 (2003) 5005–5014.
[101] D. Koulougliotis, J.B. Innes, G.W. Brudvig, Location of chlorophyll$_Z$ in photosystem II, Biochemistry 33 (1994) 11814–11822.
[102] Y. Kodera, H. Hara, A.V. Astashkin, A. Kawamori, T.-A. Ono, EPR study of trapped tyrosine Z^+ in Ca-depleted photosystem II, Biochim. Biophys. Acta Bioenerg. 1232 (1995) 43–51.
[103] K. Shigemori, H. Hara, A. Kawamori, K. Akabori, Determination of distances from tyrosine D to Q_A and chlorophyll$_Z$ in photosystem II studied by '2 + 1' pulsed EPR, Biochim. Biophys. Acta Bioenerg. 1363 (1998) 187–198.
[104] M. Tonaka, A. Kawamori, H. Hara, A. Astashkin, Three-dimensional structure of electron transfer components in photosystem II: "2 + 1" ESE of chlorophyll Z and tyrosine D, Appl. Magn. Reson. 19 (2000) 141–150.
[105] D. Koulougliotis, X.-S. Tang, B.A. Diner, G.W. Brudvig, Spectroscopic evidence for the symmetric location of tyrosines D and Z in photosystem II, Biochemistry 34 (1995) 2850–2856.
[106] A.V. Astashkin, H. Hara, A. Kawamori, The pulsed electron-electron double resonance and "2 + 1" electron spin echo study of the oriented oxygen-evolving and Mn-depleted preparations of photosystem II, J. Chem. Phys. 108 (1998) 3805–3812.
[107] A. Kawamori, N. Katsuta, H. Mino, A. Ishii, J. Minagawa, T.A. Ono, Positions of Q_A and Chl$_Z$ relative to tyrosine Y_Z and Y_D in photosystem II studied by pulsed EPR, J. Biol. Phys. 28 (2002) 413–426.
[108] A.V. Astashkin, Y. Kodera, A. Kawamori, Distance between tyrosines Z^+ and D^+ in plant photosystem II as determined by pulsed EPR, Biochim. Biophys. Acta Bioenerg. 1187 (1994) 89–93.
[109] Y. Deligiannakis, J. Hanley, A.W. Rutherford, Carotenoid oxidation in photosystem II: 1D- and 2D-electron spin-echo modulation study, J. Am. Chem. Soc. 122 (2000) 400–401.
[110] R.J. van Dorssen, J. Breton, J.J. Plijter, K. Satoh, H.J. van Gorkom, J. Amesz, Spectroscopic properties of the reaction center and of the 47 kDa chlorophyll protein of photosystem II, Biochim. Biophys. Acta Bioenerg. 893 (1987) 267–274.
[111] S.L.S. Kwa, W.R. Newell, R. van Grondelle, J.P. Dekker, The reaction center of photosystem II studied with polarized fluorescence spectroscopy, Biochim. Biophys. Acta Bioenerg. 1099 (1992) 193–202.
[112] S.V. Ruffle, D. Donnelly, T.L. Blundell, J.H.A. Nugent, A three-dimensional model of the photosystem II reaction centre of *Pisum sativum*, Photosynth. Res. 34 (1992) 287–300.
[113] J.P.M. Schelvis, P.I. van Noort, T.J. Aartsma, H.J. van Gorkom, Energy transfer, charge separation and pigment arrangement in the reaction center of photosystem II, Biochim. Biophys. Acta Bioenerg. 1184 (1994) 242–250.
[114] F. Vacha, D.M. Joseph, J.R. Durrant, A. Telfer, D.R. Klug, J. Barber, Photochemistry and spectroscopy of a five-chlorophyll reaction center of photosystem II isolated by using a Cu affinity column, Proc. Natl. Acad. Sci. U. S. A. 92 (1995) 2929–2933.
[115] A.Y. Mulkidjanian, D.A. Cherepanov, M. Haumann, W. Junge, Photosystem II of green plants: topology of core pigments and redox cofactors as inferred from electrochromic difference spectra, Biochemistry 35 (1996) 3093–3107.
[116] R.S. Hutchinson, R.T. Sayre, Site-specific mutagenesis at histidine 118 of the photosystem II D1 protein of *Chlamydomonas reinhardtii*, in: P. Mathis (Ed.), Photosynthesis: From Light to Biosphere, vol. 1, Kluwer Academic Publishers, Dordrecht, 1995, pp. 471–474.
[117] M.T. Lince, W. Vermaas, Association of His117 in the D2 protein of photosystem II with a chlorophyll that affects excitation-energy transfer efficiency to the reaction center, Eur. J. Biochem. 256 (1998) 595–602.
[118] H.G. Johnston, J. Wang, S.V. Ruffle, R.T. Sayre, T.L. Gustafson, Fluorescence decay kinetics of wild type and D2-H117N mutant photosystem II reaction centers isolated from *Chlamydomonas reinhardtii*, J. Phys. Chem. B 104 (2000) 4777–4781.
[119] H.B. Pakrasi, W.F.J. Vermaas, Protein engineering of photosystem II, in: J. Barber (Ed.), The Photosystems: Structure, Function, and Molecular Biology, vol. 11, Elsevier, Amsterdam, 1992, pp. 231–256.
[120] G. Shen, J.J. Eaton-Rye, W.F.J. Vermaas, Mutation of histidine residues in CP47 leads to destabilization of the photosystem II complex and to impairment of light energy transfer, Biochemistry 32 (1993) 5109–5115.
[121] D.H. Stewart, A. Cua, D.A. Chisholm, B.A. Diner, D.F. Bocian, G.W. Brudvig, Identification of histidine 118 in the D1 polypeptide of photosystem II as the axial ligand to chlorophyll Z, Biochemistry 37 (1998) 10040–10046.
[122] J. Wang, D. Gosztola, S.V. Ruffle, C. Hemann, M. Seibert, M.R. Wasielewski, R. Hille, T.L. Gustafson, R.T. Sayre, Functional asymmetry of photosystem II D1 and D2 peripheral chlorophyll mutants of *Chlamydomonas reinhardtii*, Proc. Natl. Acad. Sci. U. S. A. 99 (2002) 4091–4096.
[123] S.V. Ruffle, J. Wang, H.G. Johnston, T.L. Gustafson, R.S. Hutchison, J. Minagawa, A. Crofts, R.T. Sayre, Photosystem II peripheral accessory chlorophyll mutants in *Chlamydomonas reinhardtii*. biochemical characterization and sensitivity to photo-inhibition, Plant Physiol. 127 (2001) 633–644.
[124] Y. Kitajima, T. Noguchi, Photooxidation pathway of chlorophyll Z in photosystem II as studied by Fourier transform infrared spectroscopy, Biochemistry 45 (2006) 1938–1945.
[125] B. Hankamer, E. Morris, J. Nield, C. Gerle, J. Barber, Three-dimensional structure of the photosystem II core dimer of higher plants determined by electron microscopy, J. Struct. Biol. 135 (2001) 262–269.
[126] J. Nield, O. Kruse, J. Ruprecht, P. da Fonseca, C. Büchel, J. Barber, Three-dimensional structure of *Chlamydomonas reinhardtii* and *Synechococcus elongatus* photosystem II complexes allows for comparison of their oxygen-evolving complex organization, J. Biol. Chem. 275 (2000) 27940–27946.
[127] J. Nield, E.V. Orlova, E.P. Morris, B. Gowen, M.v. Heel, J. Barber, 3D map of the plant photosystem II supercomplex obtained by cryoelectron microscopy and single particle analysis, Nat. Struct. Mol. Biol. 7 (2000) 44–47.
[128] B. Hankamer, E.P. Morris, J. Barber, Revealing the structure of the oxygen-evolving core dimer of photosystem II by cryoelectron crystallography, Nat. Struct. Mol. Biol. 6 (1999) 560–564.
[129] K.-H. Rhee, E.P. Morris, J. Barber, W. Kühlbrandt, Three-dimensional structure of the plant photosystem II reaction centre at 8 Å resolution, Nature 396 (1998) 283–286.
[130] K.-H. Rhee, E.P. Morris, D. Zheleva, B. Hankamer, W. Kühlbrandt, J. Barber, Two-dimensional structure of plant photosystem II at 8-Å resolution, Nature 389 (1997) 522–526.
[131] A. Zouni, H.-T. Witt, J. Kern, P. Fromme, N. Krauss, W. Saenger, P. Orth, Crystal structure of photosystem II from *Synechococcus elongatus* at 3.8 Å resolution, Nature 409 (2001) 739–743.
[132] N. Kamiya, J.-R. Shen, Crystal structure of oxygen-evolving photosystem II from *Thermosynechococcus vulcanus* at 3.7-Å resolution, Proc. Natl. Acad. Sci. U. S. A. 100 (2003) 98–103.
[133] K.N. Ferreira, T.M. Iverson, K. Maghlaoui, J. Barber, S. Iwata, Architecture of the photosynthetic oxygen-evolving center, Science 303 (2004) 1831–1838.
[134] J. Biesiadka, B. Loll, J. Kern, K.-D. Irrgang, A. Zouni, Crystal structure of cyanobacterial photosystem II at 3.2 Å resolution: a closer look at the Mn-cluster, Phys. Chem. Chem. Phys. 6 (2004) 4733–4736.
[135] B. Loll, J. Kern, W. Saenger, A. Zouni, J. Biesiadka, Towards complete cofactor arrangement in the 3.0 Å resolution structure of photosystem II, Nature 438 (2005) 1040–1044.
[136] J. Kern, B. Loll, A. Zouni, W. Saenger, K.-D. Irrgang, J. Biesiadka, Cyanobacterial photosystem II at 3.2 Å resolution — the plastoquinone binding pockets, Photosynth. Res. 84 (2005) 153–159.
[137] J.W. Murray, K. Maghlaoui, K. Joanna, I. Naoko, T.-L. Lai, A.W. Rutherford, M. Sugiura, A. Boussac, J. Barber, X-ray crystallography identifies two chloride binding sites in the oxygen-evolving centre of photosystem II, Energy Environ. Sci. 1 (2008) 161–166.
[138] A. Guskov, J. Kern, A. Gabdulkhakov, M. Broser, A. Zouni, W. Saenger, Cyanobacterial photosystem II at 2.9-Å resolution and the role of quinones, lipids, channels and chloride, Nat. Struct. Mol. Biol. 16 (2009) 334–342.
[139] K. Kawakami, Y. Umena, N. Kamiya, J.-R. Shen, Location of chloride and its possible functions in oxygen-evolving photosystem II revealed by X-ray crystallography, Proc. Natl. Acad. Sci. U. S. A. 106 (2009) 8567–8572.
[140] M. Broser, A. Gabdulkhakov, J. Kern, A. Guskov, F. Müh, W. Saenger, A. Zouni, Crystal structure of monomeric photosystem II from *Thermosynechococcus elongatus* at 3.6-Å resolution, J. Biol. Chem. 285 (2010) 26255–26262.
[141] F. Müh, T. Renger, A. Zouni, Crystal structure of cyanobacterial photosystem II at 3.0 Å resolution: a closer look at the antenna system and the small membrane-intrinsic subunits, Plant Physiol. Biochem. 46 (2008) 238–264.
[142] H. Ishikita, E.-W. Knapp, Redox potentials of chlorophylls and β-carotene in the antenna complexes of photosystem II, J. Am. Chem. Soc. 127 (2005) 1963–1968.
[143] C.A. Tracewell, G.W. Brudvig, Multiple redox-active chlorophylls in the secondary electron-transfer pathways of oxygen-evolving photosystem II, Biochemistry 47 (2008) 11559–11572.
[144] B. Loll, J. Kern, W. Saenger, A. Zouni, J. Biesiadka, Lipids in photosystem II: interactions with protein and cofactors, Biochim. Biophys. Acta Bioenerg. 1767 (2007) 509–519.
[145] S. Vasil'ev, P. Orth, A. Zouni, T.G. Owens, D. Bruce, Excited-state dynamics in photosystem II: insights from the X-ray crystal structure, Proc. Natl. Acad. Sci. U. S. A. 98 (2001) 8602–8607.
[146] S. Vasil'ev, G.W. Brudvig, D. Bruce, The X-ray structure of photosystem II reveals a novel electron transport pathway between P680, cytochrome b_{559} and the energy-quenching cation, Chl$_Z^+$, FEBS Lett. 543 (2003) 159–163.
[147] H. Ishikita, B. Loll, J. Biesiadka, J. Kern, K.-D. Irrgang, A. Zouni, W. Saenger, E.-W. Knapp, Function of two β-carotenes near the D1 and D2 proteins in photosystem II dimers, Biochim. Biophys. Acta Bioenerg. 1767 (2007) 79–87.
[148] P. Faller, A.W. Rutherford, R.J. Debus, Tyrosine D oxidation at cryogenic temperature in photosystem II, Biochemistry 41 (2002) 12914–12920.
[149] P. Cardol, G. Forti, G. Finazzi, Regulation of electron transport in microalgae, Biochim. Biophys. Acta Bioenergetics 1807 (2011) 912–918.

[150] W. Onno Feikema, M.A. Marosvögyi, J. Lavaud, H.J. van Gorkom, Cyclic electron transfer in photosystem II in the marine diatom *Phaeodactylum tricornutum*, Biochim. Biophys. Acta Bioenerg. 1757 (2006) 829–834.
[151] P.J. Nixon, F. Michoux, J. Yu, M. Boehm, J. Komenda, Recent advances in understanding the assembly and repair of photosystem II, Ann. Bot. Lond. 106 (2010) 1–16.
[152] C.C. Moser, C.C. Page, P. Leslie Dutton, Tunneling in PSII, Photochem. Photobiol. 4 (2005) 933–939.
[153] Q. Tan, D. Kuciauskas, S. Lin, S. Stone, A.L. Moore, T.A. Moore, D. Gust, Dynamics of photoinduced electron transfer in a carotenoid–porphyrin–dinitronaphthalenedicarboximide molecular triad, J. Phys. Chem. B 101 (1997) 5214–5223.
[154] D.C. Borg, J. Fajer, R.H. Felton, D. Dolphin, The π-cation radical of chlorophyll *a*, Proc. Natl. Acad. Sci. U. S. A. 67 (1970) 813–820.
[155] Y. Gao, K.E. Shinopoulos, C.A. Tracewell, A.L. Focsan, G.W. Brudvig, L.D. Kispert, Formation of carotenoid neutral radicals in photosystem II, J. Phys. Chem. B 113 (2009) 9901–9908.
[156] T. Okubo, T. Tomo, T. Noguchi, Detection of the D0→D1 transition of β-carotene radical cation photoinduced in photosystem II, Photochem. Photobiol. 8 (2009) 157–161.
[157] J. De Las Rivas, A. Telfer, J. Barber, Two coupled β-carotene molecules protect P680 from photodamage in isolated Photosystem II reaction centres, Biochim. Biophys. Acta Bioenerg. 1142 (1993) 155–164.
[158] C.A. Tracewell, G.W. Brudvig, Two redox-active β-carotene molecules in photosystem II, Biochemistry 42 (2003) 9127–9136.
[159] C. Tracewell, G. Brudvig, Characterization of the secondary electron-transfer pathway intermediates of photosystem II containing low-potential cytochrome b_{559}, Photosynth. Res. 98 (2008) 189–197.
[160] P. Faller, A. Pascal, A.W. Rutherford, β-Carotene redox reactions in photosystem II: electron transfer pathway, Biochemistry 40 (2001) 6431–6440.
[161] A. Telfer, S. Dhami, S.M. Bishop, D. Phillips, J. Barber, β-Carotene quenches singlet oxygen formed by isolated photosystem II reaction centers, Biochemistry 33 (1994) 14469–14474.
[162] J.B. Arellano, S. González-Pérez, F. Vacha, T.B. Melø, K.R. Naqvi, Reaction center of photosystem II with no peripheral pigments in D2 allows secondary electron transfer in D1, Biochemistry 46 (2007) 15027–15032.
[163] R. Litvin, D. Bina, F. Vacha, Room temperature photooxidation of β-carotene and peripheral chlorophyll in photosystem II reaction centre, Photosynth. Res. 98 (2008) 179–187.
[164] E. Schlodder, T. Renger, G. Raszewski, W.J. Coleman, P.J. Nixon, R.O. Cohen, B.A. Diner, Site-directed mutations at D1-Thr179 of photosystem II in *Synechocystis* sp. PCC 6803 modify the spectroscopic properties of the accessory chlorophyll in the D1-branch of the reaction center, Biochemistry 47 (2008) 3143–3154.
[165] J.A. Bautista, C.A. Tracewell, E. Schlodder, F.X. Cunningham, G.W. Brudvig, B.A. Diner, Construction and characterization of genetically modified *Synechocystis* sp. PCC 6803 photosystem II core complexes containing carotenoids with shorter π-conjugation than β-carotene, J. Biol. Chem. 280 (2005) 38839–38850.